Astron. Astrophys. 351, 147–155 (1999)

ASTRONOMY AND ASTROPHYSICS

Outbursts in symmetric sources: the case of the galactic jet GRS 1915+105

C. García-Miró[1,2], **J.L. Gómez**[2], **and A. Alberdi**[1,2]

[1] Laboratorio de Astrofísica Espacial y Física Fundamental, INTA, Apdo. 50727, 28080 Madrid, Spain
[2] Instituto de Astrofísica de Andalucía, CSIC, Apdo. 3004, 18080 Granada, Spain

Received 3 March 1999 / Accepted 15 September 1999

Abstract. We present a model to study the evolution of pair components moving in symmetric jets. The model fits the observed components flux ratio evolution obtaining the geometric (sizes, opening angles, system orientation with respect to the observer) and kinematic (speeds, expansion velocities) properties of the system. We have applied the model to the pair of components originated by the prominent radio flare emitted by the galactic source GRS 1915+105 in March 1994, and described in Mirabel & Rodríguez (1994). We have found an asymmetry between the approaching and receding jets which implies a slower expansion velocity of the receding component and may account for the slower steepening of its spectrum necessary to fit our model. Each component is found to have similar longitudinal and transverse expansion velocities.

Key words: relativity – stars: individual: GRS 1915+105 – ISM: jets and outflows – radio continuum: stars

1. Introduction

The discovery of microquasars, galactic objects with similar characteristics to those seen in quasars, has provided a new approach to the problem of accreting compact objects with relativistic jets. The similarity between them is not only morphological, with a "two sided jet-disk" like structure. Other shared characteristics, such as high energy spectra and relativistic jets with apparent superluminal motion, also support a physical analogy (Mirabel & Rodríguez 1994, 1998, 1999; Falcke & Biermann 1996; Harmon 1998).

The X-ray transient source GRS 1915+105, discovered by Castro-Tirado et al. (1992), was the first galactic object in which superluminal motion was observed during a major radio outburst (Mirabel & Rodríguez 1994). Since then, GRS 1915+105 has experienced several outbursts of different intensities (Rodríguez & Mirabel 1999), such as the one recently reported by Fender et al. (1998) and mapped with higher angular resolution using the MERLIN interferometer. Superluminal motion has also been detected in other galactic sources, such as GRO J1655-40 (Tingay et al. 1995; Hjellming & Rupen 1995). Several other galactic sources also exhibit collimated radio jets, and are considered to be mildly relativistic, such as the well known SS433 (Hjellming & Johnston 1981), GRS 1758-258 (Mirabel 1994), and 1E1740-2942 (Chen et al. 1994). A detailed review and description of galactic sources with relativistic jets can be found in Mirabel & Rodríguez (1999).

Simultaneous multi-wavelength observations have been carried out to study the relationship between the jet formation and the accretion of matter onto the compact object, presumably a stellar black hole or neutron star (Mirabel et al. 1998; Eikenberry et al. 1998). These observations show a clear connection between all the wavelength bands, from γ-rays to radio. Strong IR-radio outbursts are related with large outbursts and sudden drops in hard X-rays. Besides these outbursts, they also present a large variety of quasi-periodic oscillations in the X-ray band that seem to be related with accretion onto a black hole (Harmon 1998, and references therein).

The study of microquasars has some advantages with respect to their extragalactic relatives. Thanks to their proximity and stellar size, we can study the processes related with the accretion, formation, collimation, and propagation of relativistic jets in much shorter timescales than for their extragalactic counterparts.

The detection of a pair component ejection in the jet and counter-jet of GRS 1915+105 allowed Mirabel & Rodríguez (1994) to obtain a determination of the angle through which the jets are observed ($70 \pm 2^\circ$), as well as the moving pattern speed ($0.92 \pm 0.08\,c$), assuming that components are symmetric blobs of material. The disagreement between the observed, approximated constant, flux ratio (8 ± 1) and its theoretical value expected for symmetric blobs (~ 12), led Bodo & Ghisellini (1995) to consider a shock nature for the components, obtaining a velocity for the emitting fluid ($0.73\ c$). On the contrary, Atoyan & Aharonian (1997) extended the blob model to allow asymmetric ejections in orientation, luminosity and speed, reproducing the observed flux ratio with a small asymmetry between the jets. A recent model by Atoyan & Aharonian (1999) reproduces the observed flux density evolution considering adiabatic, radiative and energy dependent losses, together with a continuous injection of relativistic electrons. A symmetric blob model was also applied by Hjellming & Rupen (1995) to inter-

Send offprint requests to: C. García-Miró

pret their observations on GRO J1655-40, obtaining the angle to the line of sight ($85 \pm 2^\circ$) and the ejecta speed ($0.92 \pm 0.02\,c$).

In this paper we present a model to study outbursts in symmetric sources, extending previous work to allow the generation of asymmetric components in size, speed, expansion velocity, and spectral index evolution. The model calculates the emission from the pair of bright components, which may be considered as blobs of material or moving shocks, taking into account all the available observational data from the outburst, not only the proper motions, but also the components sizes and spectral index evolutions. We have applied this asymmetric model to the GRS 1915+105 prominent radio flare described in Mirabel & Rodríguez (1994) reproducing the observed variability in the flux ratio, obtaining further information about the separate components evolution.

2. Model description

We assume that these sources have a symmetric jet-counter jet structure, oriented at an angle θ with respect to the line of sight. At the jet inlet, both jets are assumed to share the same physical properties (i.e., electron density, magnetic field strength and orientation) and to expand adiabatically. We allow the jets to have different opening angles, which may result in a different evolution of the physical parameters along each jet. Outbursts in the emission of these sources are considered to be related with the generation of a pair of bright components moving along the jets. We allow them to be asymmetric, hence to differ in propagation speeds, sizes, and expansion velocities, but with the same initial physical properties corresponding to the jet inlet.

Several interpretations have been proposed for the nature of the bright components observed in these sources, usually in terms of blobs of material ejected in opposite directions (Mirabel & Rodríguez 1994, 1998; Mirabel et al. 1998; Atoyan & Aharonian 1997), or shock waves propagating downstream the jets (Bodo & Ghisellini 1995). These two interpretations have been considered in our model and we will use the term "component" referring to both cases indistinctly.

We assume a conical geometry for both jets, as well as for the components. In the case of blobs, this geometry is considered to be generated by multiple ejections of components, sweeping out the external medium, creating (conical) funnels through which the blobs travel. For the shock case, we assume that the shock covers the complete transverse section of the jet. Therefore components will have a truncated conical geometry and we will refer to the cone height as longitudinal size, l, parallel to the movement, and to the base diameter as transverse size, d.

Components emission is assumed to be optically thin, with a power-law spectrum and variable spectral index, to account for a steepening of the spectrum as the jet expands. As well as the other physical parameters, the spectral index may evolve differently for each component, as long as they experience an asymmetry in their overall physical parameters evolution.

Following these assumptions and considering all the available observational data from the outburst (i.e., components proper motion, observed sizes evolution, observed spectral indices evolution, estimated magnetic field strength, etc.), the model fits the components flux ratio determining the viewing angle of the system. Once the viewing angle is known, the model determines the components sizes and jet opening angles, as well as the components speeds and their expansion velocities.

In order to formulate our model we consider four different reference frames: the observer frame; the source frame, (for the particular case of galactic sources this frame can be considered at rest with respect to the observer's because of the negligible source redshift); the proper rest frame for each component (pattern frame); and the fluid rest frame. In the shock case both jets have the same jet fluid velocity but may differ in the pattern and fluid (shocked material) velocities. For the blob case the fluid and pattern frame can be identified.

From the observed proper motions for the approaching and receding components μ_a and μ_r (hereafter subindices a and r will refer to the approaching and receding jets, respectively), the speeds β_a and β_r, in the source frame can be obtained from the following equations

$$\mu_a = \frac{\beta_a \sin\theta}{1-\beta_a\cos\theta}\,\frac{c}{D} \tag{1}$$

$$\mu_r = \frac{\beta_r \sin\theta}{1+\beta_r\cos\theta}\,\frac{c}{D} \tag{2}$$

where D is the distance to the source.

The observed flux ratio $F(\omega)$ at equal angular separations ω, can be expressed in terms of the observed volumes and emission coefficients (for a given observing frequency ν^o), in the form

$$F(\omega) = \frac{F_a(\omega)}{F_r(\omega)} = \frac{V_a(\omega)}{V_r(\omega)}\,\frac{\varepsilon_a^o(\omega,\nu^o)}{\varepsilon_r^o(\omega,\nu^o)} \tag{3}$$

The volume is calculated dividing the component into thin elliptical slabs of major semi-axis $r = d/2$, i.e. half of the transverse size, and minor semi-axis

$$r\,\frac{|\cos\theta-\beta|}{1-\beta\cos\theta} \tag{4}$$

Integrating the infinitesimal volume of each slab from the initial major semi-axis value r_o to the final value $r_f = r_o + l_p\tan\phi^o$, we obtain the following expression for the observed volume

$$V = \frac{\pi}{3}\,\frac{|\cos\theta-\beta|}{1-\beta\cos\theta}(3r_o^2 l_p + 3r_o {l_p}^2\tan\phi^o + {l_p}^3\tan^2\phi^o) \tag{5}$$

where

$$l_p = \frac{\sin\theta}{1-\beta\cos\theta}\,l \tag{6}$$

is the contribution of the longitudinal size in the source frame l, to the observed one l^o, and ϕ^o corresponds to the observed half-opening angle.

The observed total linear longitudinal size l^o, is the sum of the contribution from l and the faces of the truncated cone, both affected by time delays. It can be computed for the approaching and receding components following the equations

$$l_a^o = \frac{\sin\theta}{1-\beta_a\cos\theta}\,l_a + \frac{|\cos\theta-\beta_a|}{1-\beta_a\cos\theta}\,(d_a + l_a\tan\phi_a) \tag{7}$$

$$l_r^o = \frac{\sin\theta}{1+\beta_r\cos\theta}\, l_r + \frac{\cos\theta+\beta_r}{1+\beta_r\cos\theta}\,(d_r + l_r\tan\phi_r) \quad (8)$$

Fitting the observed longitudinal sizes to the above equations, we derive l and d for each component, from which using Eqs. (6) and (5) we can compute the observed volume.

We can relate the observed emission coefficients with the coefficients in the fluid frame, for optically thin emission and power-law spectrum $S(\nu) \propto \nu^{-\alpha}$, as follows

$$\varepsilon^o(\omega,\nu^o) = (\delta^f)^{2+\alpha(\omega)}\,\varepsilon(x,\nu^o) \quad (9)$$

where δ^f is the relativistic Doppler factor of the emitting fluid and x is the lineal distance in the source frame corresponding to the observed angular distance ω

$$x_{r,a} = \frac{(1\pm\beta_{r,a}\cos\theta)D}{\sin\theta}\,\omega = \frac{\beta_{r,a}c}{\mu_{r,a}}\,\omega \quad (10)$$

where the sign '+' corresponds to the receding jet. Note that this equation is valid for $t = t^o$, i.e. source frame at rest with respect the observer frame, assumption which is valid for galactic sources.

The emission coefficient in the fluid frame depends on the electron density N_o, the magnetic field B, and the frequency ν, as follows

$$\varepsilon \propto N_o B^{\alpha+1}\nu^{-\alpha} \quad (11)$$

Assuming for the electron density and the magnetic field a generic dependence with the jet radius

$$N_o(r) = N_{oo}\left(\frac{r}{r_o}\right)^{-Y} \quad (12)$$

$$B(r) = B_o\left(\frac{r}{r_o}\right)^{-Z} \quad (13)$$

the emission coefficient can be computed as a function of the half-opening angle ϕ, and the distance x, along the conical jet with radius $r = x\,\tan\phi$

$$\varepsilon \propto N_{oo}B_o^{\alpha+1}(\tan\phi)^{-\xi}\left(\frac{x}{r_o}\right)^{-\xi}\nu^{-\alpha} \quad (14)$$

where $\xi = Y + (\alpha+1)\,Z$.

Therefore the emission coefficients ratio in the fluid frame as a function of variables computed in the fluid frame is

$$\frac{\varepsilon_a(x_a,\nu)}{\varepsilon_r(x_r,\nu)} = \frac{N_{ooa}}{N_{oor}}\frac{(B_{oa})^{\alpha_a(x_a)+1}}{(B_{or})^{\alpha_r(x_r)+1}}\frac{\nu^{-\alpha_a(x_a)}}{\nu^{-\alpha_r(x_r)}} \times\frac{(\tan\phi_a)^{-\xi_a(x_a)}}{(\tan\phi_r)^{-\xi_r(x_r)}}\frac{(x_a/r_{oa})^{-\xi_a(x_a)}}{(x_r/r_{or})^{-\xi_r(x_r)}} \quad (15)$$

Under our assumption of equal physical properties at the jet inlet, $N_{ooa} = N_{oor} = N_{oo}$ and $B_{oa} = B_{or} = B_o$.

Transforming the emission coefficient into the observer frame, and taking into account that the spectral index value at some x position is the same than in the corresponding observed position, $\alpha(x) = \alpha(\omega = \mu x/\beta c)$, the final expression for the flux ratio is

$$F(\omega) = \frac{V_a(\omega)}{V_r(\omega)}\frac{\delta_a^{f\,(2+\alpha_a(\omega))}}{\delta_r^{f\,(2+\alpha_r(\omega))}}\frac{(\delta_a)^{\xi_a(\omega)}}{(\delta_r)^{\xi_r(\omega)}}\frac{(\Gamma_a)^{\xi_a(\omega)}}{(\Gamma_r)^{\xi_r(\omega)}}\frac{(\nu^o)^{-\alpha_a(\omega)}}{(\nu^o)^{-\alpha_r(\omega)}} \times\frac{B_o{}^{(1+\alpha_a(\omega))}}{B_o{}^{(1+\alpha_r(\omega))}}\frac{r_{oa}{}^{\xi_a(\omega)}}{r_{or}{}^{\xi_r(\omega)}}\frac{\omega^{-\xi_a(\omega)}}{\omega^{-\xi_r(\omega)}}\frac{(\tan\phi_a^o)^{-\xi_a(\omega)}}{(\tan\phi_r^o)^{-\xi_r(\omega)}} \quad (16)$$

where $\xi_{a,r}(\omega) = Y + (\alpha_{a,r}(\omega)+1)\,Z$.

For the particular case of symmetric outbursts (equal sizes and velocities) and assuming a constant power-law spectrum for the components (constant and equal spectral indices), this equation simplifies to the following constant expression

$$F(\omega) = \frac{V_a(\omega)}{V_r(\omega)}\left(\frac{\delta_a^f}{\delta_r^f}\right)^{(2+\alpha)} = \left(\frac{1+\beta\cos\theta}{1-\beta\cos\theta}\right)\left(\frac{1+\beta^f\cos\theta}{1-\beta^f\cos\theta}\right)^{(2+\alpha)} \quad (17)$$

where for the ratio of observed volumes, only the relativistic effects (time delay) on the longitudinal dimension have been taken into account. This is in agreement with a previous model by Bodo & Ghisellini (1995) and for the $\beta = \beta^f$ case (equal pattern and fluid velocities), with Mirabel & Rodríguez (1994) model.

For a conical jet in adiabatic expansion, the electron density varies with the jet radius following (Hughes et al. 1989)

$$N_o(r) \propto r^{-\frac{2}{3}(2\alpha+3)} \quad (18)$$

while the magnetic field evolves as $B_\perp \propto r^{-1}$, $B_\parallel \propto r^{-2}$ for perpendicular or parallel orientations with respect to the jet axis, respectively. Assuming for 'blob' and 'shock' cases these same evolutions, the coefficient ξ can be computed using

$$\xi_{a,r}(\omega) = \frac{7}{3}\alpha_{a,r}(\omega) + 3 + \eta\,(\alpha_{a,r}(\omega)+1) \quad (19)$$

with $\eta = 0, 1$ for a perpendicular or parallel magnetic field, respectively.

The final expression for the flux ratio evolution (Eq. 16) can be applied to both, blob and shock cases. In the case of blobs, the Doppler factor for the fluid δ^f, and the component δ, would be the same.

3. Application to GRS 1915+105

The galactic microquasar GRS 1915+105 provides us with an exceptional laboratory for the study of very relativistic jets. It exhibits the usual characteristics of quasars (i.e., collimated relativistic jets, bright components with superluminal motion), and thanks to its proximity ($D = 12.5 \pm 1.5$ Kpc; Mirabel & Rodríguez 1994) and orientation, we can follow up the evolution of pair components in both, the jet and counter-jet, in timescales much smaller than in its extragalactic counterparts. The detection of components in both jets provides added information allowing us to determine the geometric and kinematic

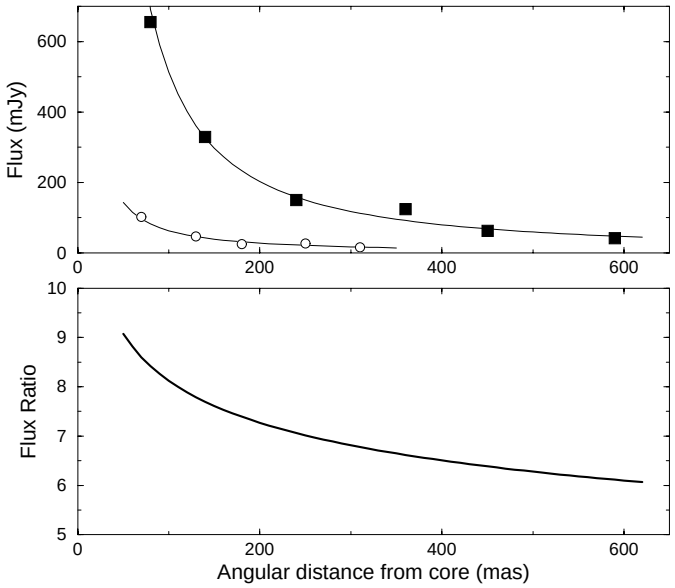

Fig. 1. Pair components (approaching -squares- and receding -circles-) observed flux evolution (*top*), and corresponding flux ratio at equal observed angular distance from core (*bottom*). Data from Table 1 of Mirabel & Rodríguez (1994).

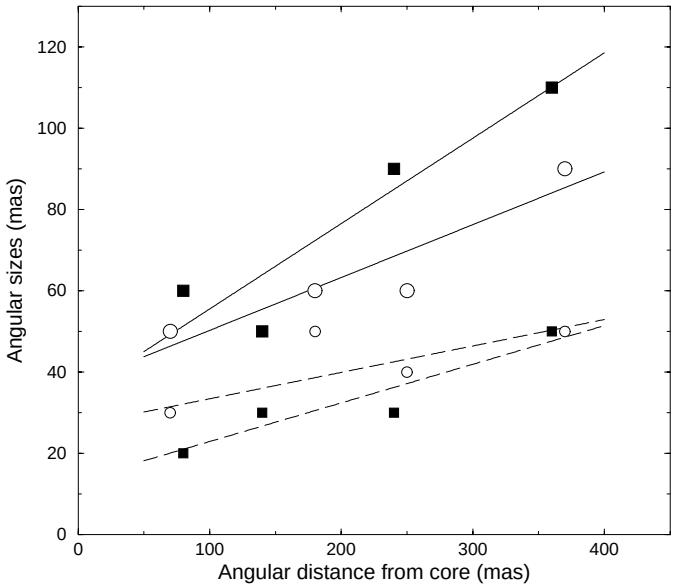

Fig. 2. Observed longitudinal (solid lines, large symbols) and transverse (dashed lines, small symbols) angular sizes for the approaching (squares) and receding (circles) components. Data from Table 1 of Mirabel & Rodríguez (1994).

properties of the source. Detailed knowledge of the components geometry and their evolution can help us to determine their nature and discern whether they are blobs of material or moving shock waves.

These properties make GRS 1915+105 an excellent candidate to test our model and try to obtain a better knowledge of the physical processes governing its evolution.

3.1. Data from observations

We have applied our model to the prominent radio flare detected in the galactic source GRS 1915+105 in March 1994, and described in Mirabel & Rodríguez (1994).

In order to constrain our model, we make use of the observational data published by Mirabel & Rodríguez (1994). In particular, our model requires: the flux ratio evolution (see Fig. 1); the components proper motions, $\mu_a = 17.6 \pm 0.4$ mas/d, and $\mu_r = 9.0 \pm 0.1$ mas/d, and their angular longitudinal and transverse sizes evolution (see Fig. 2); the estimated source distance $D = 12.5 \pm 1.5$ Kpc; the inferred magnetic field strength at the jet inlet $B = 16$ G (Mirabel et al. 1998); and the spectral index evolution (Rodríguez et al. 1995).

The flux evolution for each component is plotted in Fig. 1(top), and is best fitted by a power law decay which is typical of an optically thin adiabatic expansion, obtaining for the approaching and receding components

$$F_a(\omega) \;=\; (23.4 \pm 1.2)\,\omega^{-(1.34\pm0.10)} \tag{20}$$

$$F_r(\omega) \;=\; (4.2 \pm 1.4)\,\omega^{-(1.18\pm0.16)} \tag{21}$$

where ω is the angular distance from core in arcsec. These fits have been obtained excluding the April 30th data which seems to be affected by a new component ejection. The observed flux ratio evolution (see Fig. 1, bottom) can also be fitted to a power law in the form

$$F_{obs}(\omega) = \frac{F_a(\omega)}{F_r(\omega)} = (5.6\,\omega^{-0.16}) \;\pm\; 1 \tag{22}$$

In order to allow asymmetries in the components sizes and expansion speeds we have to consider this evolution in the flux ratio.

The evolution of the observed angular transverse and longitudinal sizes for each component is plotted in Fig. 2. Assuming a constant expansion speed for the components, we can fit the evolution to the following linear equations in the observed angular distance ω (hereafter in mas)

$$\Phi_{la}(\omega) \;=\; (0.21 \pm 0.06)\,\omega + (35 \pm 13) \tag{23}$$

$$\Phi_{lr}(\omega) \;=\; (0.13 \pm 0.04)\,\omega + (37 \pm 9) \tag{24}$$

$$\Phi_{da}(\omega) \;=\; (0.10 \pm 0.01)\,\omega + (13 \pm 3) \tag{25}$$

$$\Phi_{dr}(\omega) \;=\; (0.07 \pm 0.03)\,\omega + (27 \pm 7) \tag{26}$$

We should note that these equations are only valid for the observed range, $\omega \gtrsim 50\,mas$, which corresponds to jet regions far enough from the central engine. In these regions the jet can be considered, as a very good approximation, conical with constant flow bulk Lorentz factor. We can not extrapolate linearly the sizes to the jet origin due to the different physics which is governing the inner jet regions near to the central engine, where the jet flow bulk Lorentz factor is not constant (Marscher 1980).

These fits were obtained after excluding some of the data from Mirabel & Rodríguez (1994). For the approaching component the last three longitudinal values deviate from the first measurements behaviour, which seems to be caused by a new component ejection. This does not seem to affect the transverse

size. For the receding component we have excluded one longitudinal measurement because it would imply a decrease in size with time. As for the approaching component, all the transverse sizes have been considered. In the error analysis only the linear regression errors have been taken into account.

From the transverse sizes Φ_{da} and Φ_{dr}, we derive jet half-opening angles of $\phi_a^o = 2.73 \pm 0.01^\circ$ and $\phi_r^o = 1.87 \pm 0.03^\circ$. This asymmetry in the observed opening angles would also imply an asymmetry between the intrinsic jets under our assumption of equal angle to the line of sight (θ and $\theta + 180^\circ$) for both jets.

Rodríguez et al. (1995) measured a steepening of the components spectra as they moved downstream, from $\alpha = 0.49 \pm 0.01$ (at March 24) to $\alpha = 0.84 \pm 0.03$ (at April 16). We take into account this steepening but note that since those measurements were obtained at equal observing times (different angular separations), the components would be compared in a similar evolved state only for the case of symmetric components (with the same speed and sizes). The easiest way to cope with this small amount of information is to assume a linear evolution between the two measured values

$$\alpha_a(\omega) = (9.5 \pm 0.5) \times 10^{-4}\,\omega + 0.41 \pm 0.01 \quad (27)$$

$$\alpha_r(\omega) = (16.7 \pm 1.0) \times 10^{-4}\,\omega + 0.42 \pm 0.01 \quad (28)$$

Our model assumes an adiabatic evolution for the components. In order to test if this hypothesis can be applied to GRS 1915+105 we have obtained a rough estimation of the adiabatic and synchrotron losses, considering data from Mirabel et al. (1998) and Fender et al. (1997) and the simplest case of spheric blobs in expansion, concluding that synchrotron losses are negligible, in concordance with Mirabel et al. (1998). An alternative model by Atoyan & Aharonian (1999) considers not only adiabatic losses, but also radiative and energy-dependent losses, together with continuous supply or in-situ acceleration of radio electrons, reproducing the flux density evolution of the jets.

3.2. Resolution method

In our model we need to solve for the following unknowns: angle to the line of sight θ; components speeds β_a and β_r, and sizes l_a, d_a and l_r, d_r; and magnetic field orientation. In the case of shocks, we also need to determine the fluid velocity β^f. Since the number of unknowns is larger than the available relationships, our solutions will be a function of the magnetic field orientation (and of the fluid velocity for shocks), introduced as a free parameter.

In order to constrain our model, we need to follow an iterative process searching for the model that best fit the observational data. From the observed proper motions, we first obtain a range of allowed values for the viewing angle θ. For each viewing angle, we estimate the components velocities β_a and β_r using Eqs. (1) and (2), and hence the corresponding Doppler factors. With this, using Eq. (16) we compute the components flux ratio $F(\omega_i)$ for several angular distances (ω_i= 100, 200, 300, 400 and 500 mas).

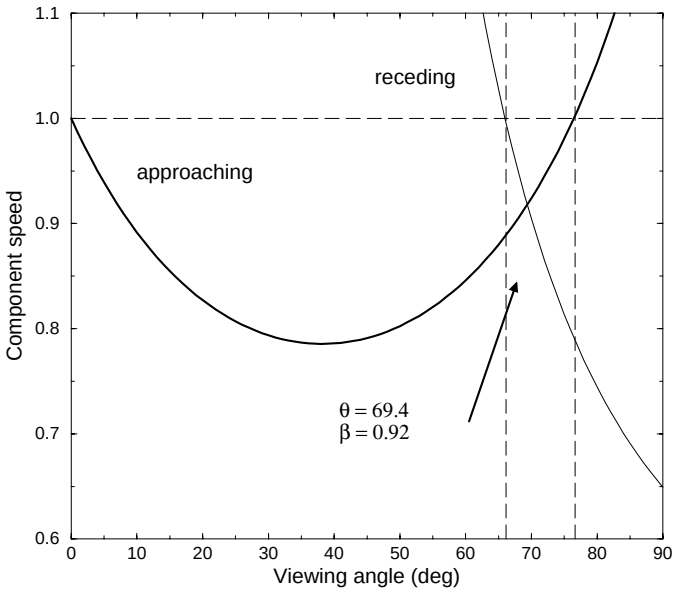

Fig. 3. Components speeds, approaching (thick line) and receding (thin line), as a function of the viewing angle showing the allowed range of θ values and the case of components with equal velocities.

In order to quantify the fit of the model to the observational data we compute the standard deviation of the model points $(\omega_i, F(\omega_i))$ with respect to the observed $F_{obs}(\omega)$ curve

$$S.D. = \left[\frac{\sum(\ln F(\omega_i) - \ln a - b \ln \omega_i)^2}{N-2}\right]^{1/2} \quad (29)$$

where a and b are the coefficients of the power law fit $F_{obs} = a\,\omega^b$ (Eq. 22).

The adopted viewing angle of the system would be that which minimizes the standard deviation. Considering a flux error determination of $\sim 5\%$, angular position error ~ 0.05 arcsec, angular resolution ~ 0.2 arcsec, we estimate an error in the determination of the viewing angle of approximately $\pm 1^\circ$. Indeterminations in the distance to GRS 1915+105 would increase this error to about $\pm 2^\circ$.

3.3. Fit of the model to the observations

Using Eqs. (1) and (2) we can obtain the range of allowed values for the viewing angle θ compatible with the observed proper motions (see Fig. 3). Note that a particular solution corresponds to the symmetric pair ejection case studied by Mirabel & Rodríguez (1994), for which both components have the same velocity of $\beta = 0.92$, viewed with $\theta = 69.4^\circ$.

The estimated components sizes obtained using Eqs. (7) and (8) differs for the approaching and receding components, indistinctly of the value of θ we choose within the allowed range. This implies, even for the case of equal components velocity, an intrinsic asymmetry in the pair of components, resulting in a different time evolution of their physical properties.

For simplicity, in this paper, and in order to apply our model to the March 1994 radio flare in GRS 1915+105, we have restricted ourselves to the "blob case". This also allows a better

comparison with previous models. We discuss some aspects of the "shock case" in Sect. 4. In our model, one of the parameters that most strongly determines the solution is the spectral index. For that, and using the method described in Sect. 3.2, we have computed the standard deviation (hereafter fit error) for the modeled flux ratio as a function of θ, for parallel and perpendicular magnetic fields, and for three different evolutions of the components spectral index

- case A: linear interpolation using the observed values (Eqs. 27 and 28), which would be valid only for a completely symmetric system.
- case B: constant value of $\alpha_a = \alpha_r = 0.84$.
- case C: equal values for the approaching and receding components, both following the evolution determined for the approaching component (Eq. 27). This same evolution of both spectral indices with the observed angular distance implies an asymmetric system.

The error of the fit for each case, and as a function of the viewing angle, is plotted in Fig. 4. All three cases show a minimum in the error for a given θ and magnetic field configuration. This angle which minimizes the error is considered as the viewing angle solution for each case. The comparison of the modeled and observed flux ratios for these three cases (considering for each one the different viewing angle solution) is plotted in Fig. 5.

Case A does not fit the observed flux ratio evolution, as its large fit error (Fig. 4) indicates. The expected flux ratio for this case would increase as does the angular distance of the components, in contradiction with the observed behaviour. This poor fit for case A implies that the components can not be completely symmetric. This was actually expected, once we found the geometric asymmetry between the components. For an equal and constant spectral index for both components, case B, the fit is considerably better than for case A (see Fig. 4), but although the modeled flux ratio decreases with the observed angular distance (see Fig. 5), still the flux ratio evolution differs significantly from the observed one.

For case C, Fig. 4 shows a significantly smaller fit error than for the previous two cases. In this case we can reproduce the observed flux ratio (see Fig. 5), supporting the idea of an asymmetric outburst. For a perpendicular magnetic field the obtained viewing angle is $\theta \sim 70.3 \pm 1.0^\circ$ with components velocities $\beta_a = 0.93 \pm 0.01$ and $\beta_r = 0.90 \pm 0.02$, while for a parallel magnetic field, the angle is $\theta \sim 69.4 \pm 1.0^\circ$, very close to the symmetric speed angle, with essentially equal velocities ($\beta \sim 0.92$). The fit error is smaller for the perpendicular orientation coinciding with Atoyan & Aharonian (1999) results, although the large viewing angle errors do not allow us to discriminate between both configurations. Therefore our model cannot provide further information about the magnetic field structure within the components of GRS 1915+105. Recent polarization images by Fender et al. (1998) show a complicate behaviour of the magnetic field, with rotation of the polarization vectors in the approaching component, and depolarization of the core and receding component, from which a clear magnetic field structure cannot be inferred.

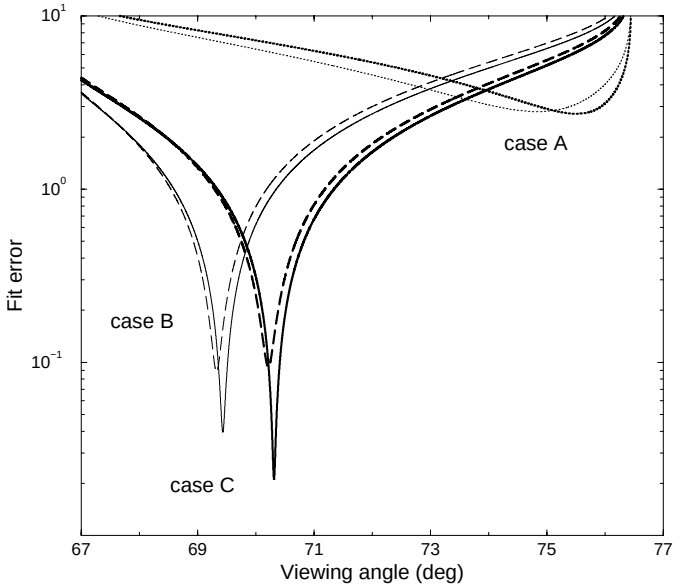

Fig. 4. Fit error as a function of the viewing angle for different spectral index evolutions: cases A (dotted lines), B (dashed lines) and C (solid lines), for parallel (thin lines) and perpendicular (thick lines) magnetic field orientations. See text for details.

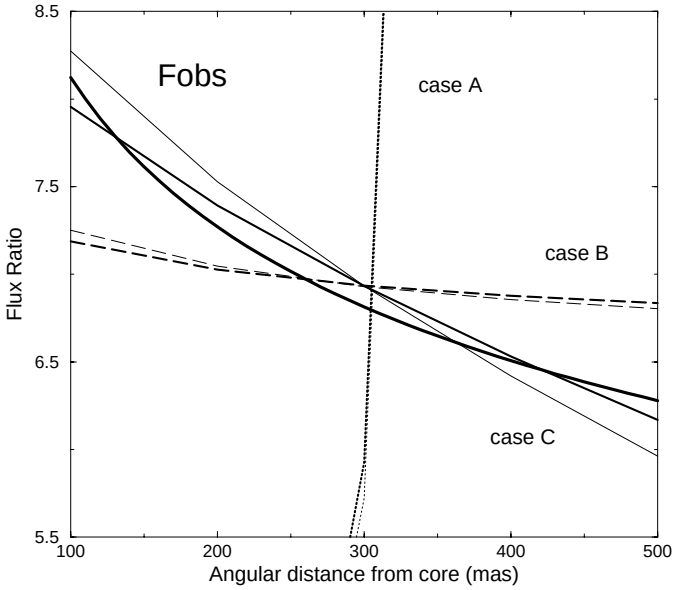

Fig. 5. Observed F_{obs} (thickest line) and modeled flux ratio for different spectral index evolutions: cases A (dotted lines), B (dashed lines) and C (solid lines), for parallel (thin lines) and perpendicular (thick lines) magnetic field orientations.

3.4. Equal components velocities

An interesting case to study, because of its simplicity and direct comparison with previous results, is the case of equal components velocities. As for the case of different velocities, we cannot obtain a good fit for cases A and B. The best fit is obtained considering the observed spectral index evolution for the approaching component (Eq. 27) and adjusting the spectral index for the receding component as to minimize the fit error. We

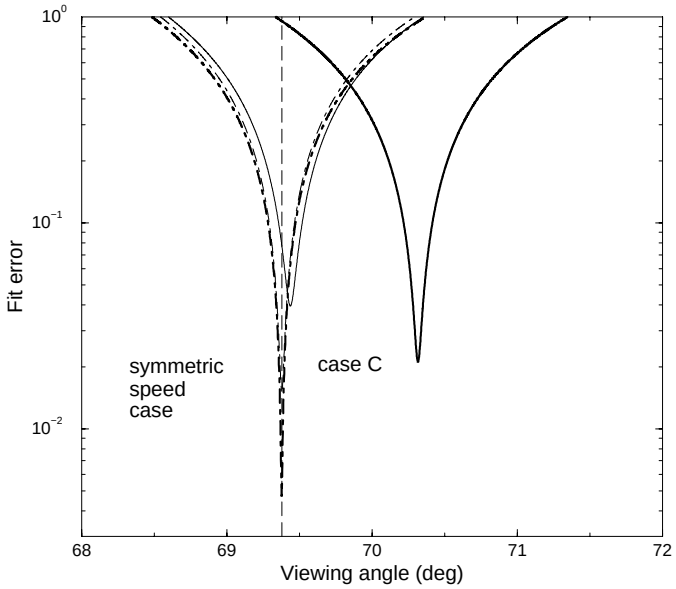

Fig. 6. Fit error as a function of the viewing angle for case C (solid lines) and the best fit obtained for equal components velocities (dot-dashed lines), for parallel (thin lines) and perpendicular (thick lines) magnetic field orientations.

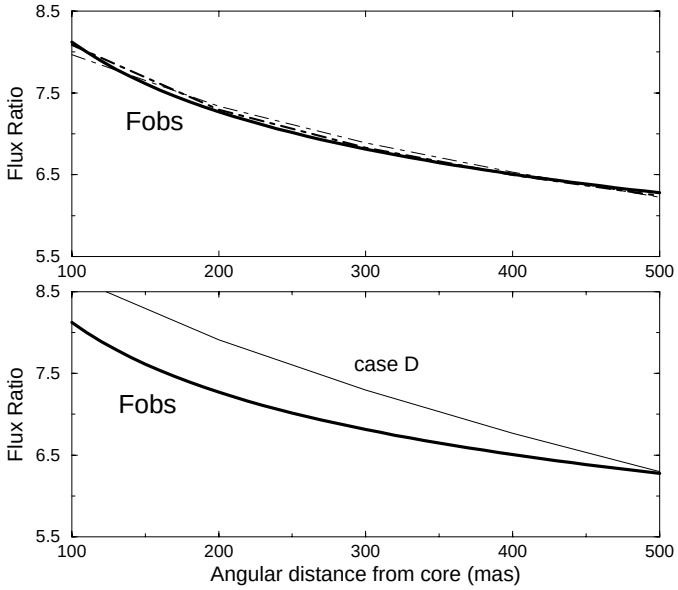

Fig. 7. Observed F_{obs} (thickest line) and modeled flux ratio for (*top*) the best fit obtained for equal components velocities (dot-dashed lines) and (*bottom*) case D. Both figures for parallel (thin lines) and perpendicular (thick lines) magnetic field orientations. Note that case D for perpendicular magnetic field is beyond the plotted range.

obtain basically the same solution indistinctly of the magnetic field orientation, with

$$\alpha_r(\omega) = (9.6 \pm 0.5) \times 10^{-4}\,\omega + 0.4 \pm 0.1 \tag{30}$$

The errors in the spectral index have been estimated taking into account the errors in the observed volume and the indetermination in the distance. Other errors are negligible compared with these. Fig. 6 shows the fit error for this symmetric speed case, and compares with the obtained for case C. The comparison between the observed flux ratio evolution and the obtained for the symmetric speed case is plotted in Fig. 7, (*top*). Evolutions of the spectral index for the receding component differing from the given in Eq. (30) result in very poor fits. For instance, Fig. 7, (*bottom*) shows the flux ratio evolution obtained for case D, corresponding to the case in which we consider the evolution of α_r given by Eq. (28), that is, case C, but with equal components velocities. For this case, the parallel magnetic field orientation results in an better fit than the other configuration, but in any case the fit is worse than in previous asymmetric models.

Therefore, in order to obtain a reasonable fit for the case of equal velocities we need to assume that the receding spectral index component evolves (increases) more slowly than for the approaching one. We can obtain similar fits fixing the evolution of the receding component as the one given by Eq. (28) and finding the appropriate evolution for the approaching component as to obtain the best fit. In any case, we obtain a slower increase in the spectral index for the receding component.

For this case of equal components velocities, independently of the evolution of the spectral indices, we can obtain estimations of the components sizes, and their evolution with time. From Eqs. (7) and (8) we obtain in the source's frame

$$l_a(x) = (0.13 \pm 0.08)\,x + 0.0010 \pm 0.0004 \tag{31}$$

$$d_a(x) = (0.13 \pm 0.01)\,x + 0.0008 \pm 0.0003 \tag{32}$$

$$l_r(x) = (0.07 \pm 0.01)\,x + 0.0009 \pm 0.0001 \tag{33}$$

$$d_r(x) = (0.05 \pm 0.02)\,x + 0.0016 \pm 0.0006 \tag{34}$$

where x is the linear distance in the source's frame (in pc). The corresponding valid range for these equations is $x \gtrsim 2 \times 10^{-3}\,pc$. These linear fits are plotted in Fig. 8, (*top*). The errors have been estimated from the observed sizes and viewing angle errors.

The sizes obtained for the beginning of the conical region ($x \sim 2 \times 10^{-3}\,pc$) are very similar for each dimension, except for the receding transverse size, which is significantly larger. The dimension of the clouds estimated by Mirabel et al. (1998), 15 minutes after the ejection, are two orders of magnitude smaller than these initial sizes, calculated several days after the ejection ($\sim 10^{13}$ cm against our $\sim 10^{15}$ cm). We can derive the jets half-opening angles from the transverse sizes evolution, obtaining $\phi_a = 2.55 \pm 0.04^\circ$ and $\phi_r = 1.74 \pm 0.05^\circ$. The expansion speeds in the source's frame differ for each component, with values $v_{la} = 0.12 \pm 0.05\,c$ and $v_{da} = 0.12 \pm 0.02\,c$ for the approaching blob; and $v_{lr} = 0.06 \pm 0.02\,c$ and $v_{dr} = 0.04 \pm 0.02\,c$ for the receding. Previous estimations considered expansion values of the order $\sim 0.2\,c$ (Mirabel et al. 1998) and $\geq (0.1 - 0.2)\,c$ (Atoyan & Aharonian 1999).

In order to understand the derived spectral indices behaviour (Eqs. 27 and 30) we have calculated their evolution with the source frame distance (see Fig. 8, *bottom*)

$$\alpha_a(x) = (22 \pm 1)\, x + 0.4 \pm 0.1 \quad (35)$$

$$\alpha_r(x) = (11.2 \pm 0.5)\, x + 0.4 \pm 0.1 \quad (36)$$

obtaining therefore different evolutions for each spectral index as is expected for an asymmetric system. Comparing with the sizes evolution (Fig. 8, *top*), it seems clear that the spectral indices behaviour that fits the observed flux ratio, is the one that follows the sizes evolution.

In summary, we have found an asymmetry between the approaching and receding jets. The receding jet is wider at the beginning of the considered conical region than the approaching jet but its opening angle is smaller. This implies a slower expansion velocity of the receding component and accounts for the slower steepening of its spectrum necessary to fit our model.

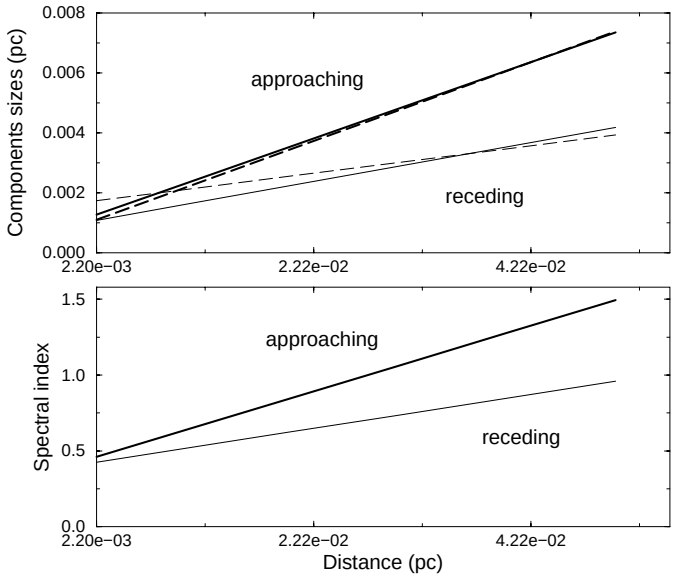

Fig. 8. *Top*: Longitudinal (solid lines) and transverse (dashed lines) sizes in the source frame for the approaching (thick lines) and receding (thin lines) components. *Bottom*: Spectral indices in the source frame. Observed evolution for approaching component (thick line) and fitted evolution for the receding component (thin line).

4. Discussion and conclusions

Several models have been considered to interpret the pair of superluminal components observed in GRS 1915+105. Mirabel & Rodríguez (1994), assuming the simplest model that provides a reasonable explanation for the observations, obtained a first estimation of the physical parameters of the source. This model assumed symmetric blobs moving with same speeds in opposite jets. However, the variation with time of the flux ratio between the approaching and receding components, as well as their different transverse (and longitudinal) expansion velocities, suggests that the outburst generated a pair of asymmetric components. We have extended Mirabel & Rodríguez (1994) model to account for this asymmetry assuming an initial condition in which both components share the same physical properties -but are allowed to have different initial sizes and evolve differently. Through a fit of the observed flux ratio by the model -for which we make use of all the available data, including the sizes evolution as well as the observed spectral evolution; we can obtain information about the intrinsic geometric and kinematic parameters of the system, which in turn allows a better interpretation of the physical processes governing the evolution of the components.

Following previous authors estimations of the electron energy losses for this modeled outburst (Mirabel et al. 1998), showing that the synchrotron losses can be neglected in comparison with the adiabatic losses, our model assumes an adiabatic conical expansion, being able to reproduce the observed flux ratio. Radiative and energy-dependent losses, as well as particle injection (Atoyan & Aharonian 1999), have not been considered in our study.

One of the parameters that most strongly determines the solution in our model is the spectral index. However very little information is available for its evolution in each component. Hence, we have considered different evolutions for the spectral index and tested which one better reproduces the observations. The model with observed spectral indices (following Eqs. 27 and 28), implying a completely symmetric system (in speeds and sizes), does not fit the flux ratio. Our best model requires both components changing its spectral index following Eq. (27), implying an asymmetric system. With this we have obtained a good fit to the data (see Fig. 5), yielding a solution for the components velocities and viewing angle, with little variation depending on the magnetic field orientation. Since the model is based on the different evolution of the physical parameters in the components, the initial common value for the magnetic field strength does not affect significantly the fit. We have used a value of $B = 16$ G as estimated by Mirabel et al. (1998), and confirmed that the used of the very different other values reported in the literature (see Fender et al. 1997, 1998; Atoyan & Aharonian 1999; Gliozzi et al. 1998) does not change the fit significantly.

In order to allow a better comparison with previous models we have also studied the case of equal components velocities. For this, none of the considered different evolutions for the spectral indices (cases A, B, and C), produce a valid solution. Therefore, we have considered an "ad hoc" spectral index evolution which fits the data (see Figs. 6 and 7), and also reflects the asymmetry of the system. We shall note that a similar "ad hoc" solution can be considered for the asymmetric case (different components velocities), but in that case different solutions can be found as a function of the viewing angle.

Indistinctly of the particular viewing angle (within the permitted range), the system is found to be asymmetric in sizes and expansion speeds, as is derived directly from the observed sizes. The result for the equal velocities case yields a similar initial (several days after ejection) longitudinal size for both components, but a significantly different transverse sizes. The

approaching component is found to expand faster (almost twice) than the receding one. This slower expansion velocity for the receding component explains why we need to assume a slower steepening for its spectrum.

Both components are found to have similar longitudinal and transverse expansion velocities in the source frame. For the case we have studied of components consisting of blobs of material moving along a jet funnel, this would represent that the ram pressure produced by the material ahead of the blobs is minimum, and hence the blobs would travel and expand through a medium with negligible pressure.

New components proper motions observed in GRS 1915+105 with high resolution (Fender et al. 1998) have revealed an upper limit for the distance to the source of 11.2 ± 0.8 Kpc. This value is within the distance error considered in this paper, and therefore the results obtained with this new estimation would not differ from the presented here.

We can apply our model to the case in which both components are associated with traveling shock waves. Then we need to introduce an extra parameter associated with the velocity of the shocked emitting plasma. The amount of information we obtain from the observations is then not enough to constrain a single model, and the final solution would be a function of the fluid velocity. However, through the study of the expansion velocities and the obtained pattern shock velocity it would be possible to obtain some estimations of the shock strength (through different assumptions about the underlying jet), and from here an initial estimation of the fluid velocity to fit a model. We are currently exploring this possibility through one dimensional relativistic hydrodynamic simulations. This, together with new observations providing detailed information about the geometric, kinematic, and emission -in particular spectral index information, should provide the necessary constrains to draw a more complete picture of the physics involved in galactic superluminal sources.

Acknowledgements. This research was supported by Spain's Dirección General de Investigación Científica y Técnica (DGICYT), grants PB94-1275 and PB97-1164. CGM gratefully acknowledge a Rafael Calvo Rodés research fellowship by the Instituto Nacional de Técnica Aeroespacial (INTA).

References

Atoyan A.M., Aharonian F.A., 1997, ApJ 490, L149
Atoyan A.M., Aharonian F.A., 1999, MNRAS 302, 253
Bodo G., Ghisellini G., 1995, ApJ 441, L69
Gliozzi M., Bodo G., Ghisellini G., 1998, accepted for publication in MNRAS as letter
Castro-Tirado A., Brandt S., Lund N., 1992, IAU Circ. 5590
Chen W., Gehrels N., Leventhal M., 1994, ApJ 426, 586
Eikenberry S.S., Matthews K., Morgan E.H., Remillard R.A., Nelson R.W., 1998, ApJ 494, L61
Falcke H., Biermann P.L., 1996, A&A 308, 321
Fender R.P., Pooley G.G., Brocksopp C., Newell S.J., 1997, MNRAS 290, L65
Fender R.P., Garrington S.T., McKay D.J., et al., 1998, accepted for publication in MNRAS
Harmon B.A., invited review article for the 3rd Integral Workshop, Taormina, Italy, September 13–18, 1998
Hjellming R., Johnston K., 1981, Nat 290, 100
Hjellming R., Rupen M., 1995, Nat 375, 464
Hughes P.A., Aller H.D., Aller M.F., 1989, ApJ 341, 54
Marscher A., 1980, ApJ 235, 386
Mirabel I.F., 1994, ApJS 92, 369
Mirabel I.F., Rodríguez L.F., 1994, Nat 371, 46
Mirabel I.F., Dhawan V., Chaty S., et al., 1998, A&A 330, L9
Mirabel I.F., Rodríguez L.F., 1998, Nat 392, 673
Mirabel I.F., Rodríguez L.F., 1999, to appear in Vol. 37 (1999) of ARA&A
Rodríguez L.F., Gerard E., Mirabel I.F., Gómez Y., Velázquez A., 1995, ApJS 101, 173
Rodríguez L.F., Mirabel I.F., 1999, to appear in ApJ
Tingay S.J., Jauncey D.L., Preston R.A., et al., 1995, Nat 374, 141